Contribution from the Laboratorium für Anorganische Chemie, ETH-Zentrum, CH-8092 Zürich, Switzerland, and
Institut für Kristallographie und Petrographie, ETH-Zentrum, CH-8092 Zürich, Switzerland

1,3,5-Triamino-1,3,5-trideoxy-*cis*-inositol, a New Ligand with a Remarkable Versatility for Metal Ions. 1. Preparation, X-ray Structure, and Stability of the Nickel(II), Copper(II), and Zinc(II) Complexes

Kaspar Hegetschweiler,*[1a] Volker Gramlich,[1b] Michele Ghisletta,[1a] and Heinz Samaras[1a]

Received December 26, 1991

Compounds of the composition $M(taci)_2(NO_3)_2{\cdot}xH_2O$ and $M(taci)_2Br_2{\cdot}xH_2O$ (M = Ni, Cu, Zn, taci = 1,3,5-triamino-1,3,5-trideoxy-*cis*-inositol, $0 \le x \le 4$) have been prepared from aqueous solution and characterized by spectroscopic methods (vis, EPR, NMR). Single-crystal X-ray analysis of $M(taci)_2Br_2{\cdot}4H_2O$ revealed an isomorphous structure for Ni(II), Cu(II), and Zn(II) with space group *Cmcm* and $Z = 4$. Ni complex: $a = 9.410$ (5) Å, $b = 11.383$ (7) Å, $c = 22.000$ (13) Å. Cu complex: $a = 9.391$ (6) Å, $b = 11.475$ (7) Å, $c = 21.924$ (12) Å. Zn complex: $a = 9.425$ (5) Å, $b = 11.431$ (6) Å, $c = 22.104$ (11) Å. In contrast to $Cr(taci)_2^{3+}$, where the ligands are coordinated to the metal via oxygen and nitrogen atoms, Ni, Cu, and Zn were exclusively bound to the three nitrogen atoms of taci, forming a MN_6 octahedron. In the case of Cu, the significant distortion corresponds to the usual Jahn-Teller effect, whereas the distortion of the Ni and Zn complexes as provoked by the crystal packing is not significant. In accordance, the NMR data showed D_{3d} symmetry for $Zn(taci)_2^{2+}$ in solution. The formation constants β_1 for $M(taci)^{2+}$ and β_2 for $M(taci)_2^{2+}$ were investigated by potentiometric titration in aqueous solution (25 °C, 0.1 M KNO_3). p*K* of taci: 5.95, 7.40, 8.90 (estimated standard deviations <0.01). Ni: $\log \beta_1 = 12.37$ (1), $\log \beta_2 = 20.94$ (1). Cu: $\log \beta_1 = 12.09$ (1), $\log \beta_2 = 18.79$ (1). Zn: $\log \beta_1 = 8.40$ (1), $\log \beta_2 = 13.56$ (1). Two minor species, $HCu(taci)_2^{3+}$ and the dimer $Cu_2(OH)_2(taci)_2^{2+}$, have also been identified. The permutation of the usual Irving Williams order is a consequence of the rigid ligand geometry which enforces facial coordination. The complex formation constants were compared with those of other triamines.

Introduction

Aliphatic and alicyclic polyamines are well-known as strong chelating agents for a variety of metals including the late transition and the IIb group elements. However, these ligands are rather inefficient regarding complex formation with hard cations like Mg(II), Ca(II), Al(III), and Fe(III). Ligands with a high affinity for almost every metal have been obtained by the combination of oxygen and nitrogen atoms in the metal-binding site. The poly(amino carboxylates) like NTA or EDTA are prominent representatives of this category. 1,3,5-Triamino-1,3,5-trideoxy-*cis*-inositol (taci) is related to the poly(amino carboxylates) since either oxygen or nitrogen atoms are available for metal binding. However, in the poly(amino carboxylates) all the nitrogen and oxygen atoms usually are coordinated to the metal ion simultaneously, whereas in taci four distinct coordination sites provide (i) three nitrogen, (ii) two nitrogen and one oxygen, (iii) one nitrogen and two oxygen, and (iv) three oxygen atoms for coordination (Chart I).

It should be realized that the distances between the ligand atoms of the axial–equatorial–axial arrangements ii and iii is somewhat longer than those in the triaxial arrangements i and iv. Therefore, the four coordination sites differ characteristically in size and softness, and it is interesting to investigate which site is selected by a distinct metal ion. taci has already been prepared in 1956 when attention was given to its structural relationship with the antibiotic streptomycin.[2] The application in coordination chemistry has been suggested by Schwarzenbach et al. in 1973.[3] However, the tedious and dangerous preparation procedure prevented a comprehensive study as a chelating agent. We recently developed an improved synthetic route to taci[4,5] and reported the structure of a Cr(III) complex where the two different isomers a and b were present in the same crystal structure in a 1:2 ratio (Chart II).[6]

In the meantime, a variety of further metals has been investigated in our laboratory. These investigations revealed clearly that taci is a very versatile ligand. Complexes of the type $M(taci)_2^{z+}$ ($M = Ca^{2+}, Ni^{2+}, Cu^{2+}, Zn^{2+}, Al^{3+}, Cr^{3+}, Co^{3+}, Ga^{3+}, Tl^{3+}, Ti^{4+}$, and Ge^{4+}) have been prepared and characterized. We intend to publish a series of papers reporting the structural properties and the reactivity of these complexes. In this contribution, we present the preparation, characterization, X-ray structure, and stability of the complexes with Ni(II), Cu(II), and Zn(II).

Chart I

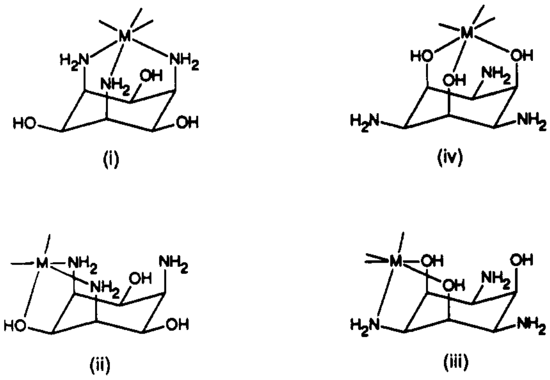

Chart II

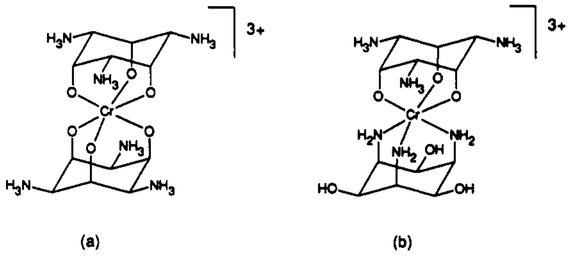

Experimental Section

Spectroscopy, Mass Spectrometry, and Analyses. The UV–vis spectra were recorded on an Uvikon 820 spectrophotometer; the ^1H and ^{13}C NMR spectra were measured on a Bruker AC-200 spectrometer with δ (ppm) scale and sodium (trimethylsilyl)propionate-d_4 (0 ppm) as internal standard. For the EPR measurements, a diluted powder sample of 1% $Cu(taci)_2Br_2{\cdot}4H_2O$ in $Zn(taci)_2Br_2{\cdot}4H_2O$ was used to obtain the spectrum recorded on a Bruker ESP 300 spectrometer (9.776 GHz) at 4 K

---

* To whom correspondence should be addressed.

(1) (a) Laboratorium für Anorganische Chemie. (b) Institut für Kristallographie und Petrographie.

(2) Quadbeck, G.; Röhm, E. *Chem. Ber.* **1956**, *89*, 1645.

(3) Schwarzenbach, G.; Bracher, G. Unpublished work, ETH Zürich, 1973.

(4) Hegetschweiler, K.; Erni, I.; Schneider, W.; Schmalle, H. *Helv. Chim. Acta* **1990**, *73*, 97.

(5) The procedure, described in ref 4, still operates with the hazardous trinitrophloroglucinol as intermediate. A more convenient pathway, using tris(phenylazo)phloroglucinoltrisulfonate as intermediate has been established in our laboratory and will be published elsewhere (manuscript in preparation).

(6) Schmalle, H. W.; Hegetschweiler, K.; Ghisletta, M. *Acta Crystallogr.* **1991**, *C47*, 2047.

0020-1669/92/1331-2341$03.00/0

Table I. Crystallographic Data for $M(taci)_2Br_2 \cdot 4H_2O$ (M = Ni, Cu, Zn)

	Ni complex	Cu complex	Zn complex
chem formula	$C_{12}H_{38}Br_2N_6NiO_{10}$	$C_{12}H_{38}Br_2CuN_6O_{10}$	$C_{12}H_{38}Br_2N_6O_{10}Zn$
fw	645.00	649.83	651.66
cryst size, mm	0.4 × 0.4 × 0.04	0.1 × 0.1 × 0.1	0.2 × 0.2 × 0.15
space group	*Cmcm* (No. 63)	*Cmcm* (No. 63)	*Cmcm* (No. 63)
cryst syst	orthorhombic	orthorhombic	orthorhombic
a, Å	9.410 (5)	9.391 (6)	9.425 (5)
b, Å	11.383 (7)	11.475 (7)	11.431 (6)
c, Å	22.000 (13)	21.924 (12)	22.104 (11)
V, Å^3	2357 (2)	2363 (2)	2381 (2)
Z	4	4	4
T, °C	17	17	17
λ(Mo Kα), Å	0.71073	0.71073	0.71073
ρ_{calcd}, g cm^{-3}	1.790	1.787	1.778
μ, cm^{-1}	42.41	43.32	44.34
transm coeff	0.2316/0.6832	0.6606/0.6965	0.4576/0.5696
$R(F_o)$,[a] %	3.54	3.28	3.65
$R_w(F_o)$,[b] %	5.80	5.22	5.36

[a] $R = \sum ||F_o| - |F_c|| / \sum |F_o|$. [b] $R_w = [\sum w(|F_o| - |F_c|)^2 / \sum w|F_o|^2]^{1/2}$, $w = 1/\sigma^2(|F_o|)$.

Table II. Atomic Coordinates and Equivalent Isotropic Temperature Factors with Estimated Standard Deviations in Parentheses for Non-Hydrogen Atoms of $M(taci)_2Br_2 \cdot 4H_2O$ (M = Ni, Cu, Zn)

atom	x	y	z	U_{eq},[a] Å^2
		Ni Complex		
Br(1)	0	0.0850 (1)	0.25	0.056 (1)
Br(2)	0	0	0	0.030 (1)
Ni	0	0.5	0	0.015 (1)
C(1)	0	0.5033 (5)	0.1573 (3)	0.026 (2)
C(2)	0.1356 (4)	0.4605 (3)	0.1266 (2)	0.020 (1)
C(3)	0.1318 (4)	0.3275 (4)	0.1191 (2)	0.024 (1)
C(4)	0	0.2830 (5)	0.0870 (3)	0.022 (2)
O(1)	0	0.6276 (4)	0.1605 (2)	0.030 (1)
O(3)	0.2545 (3)	0.2850 (3)	0.0877 (1)	0.031 (1)
N(2)	0.1573 (4)	0.5201 (3)	0.0677 (1)	0.020 (1)
N(4)	0	0.3169 (4)	0.0214 (2)	0.021 (2)
O(1W)	0	0.8934 (4)	0.1364 (3)	0.045 (2)
O(2W)	0.1843 (6)	0.7077 (6)	0.25	0.061 (2)
		Cu Complex		
Br(1)	0	0.0782 (1)	0.25	0.059 (1)
Br(2)	0	0	0	0.030 (1)
Cu	0	0.5	0	0.018 (1)
C(1)	0	0.4979 (6)	0.1566 (4)	0.026 (3)
C(2)	0.1362 (5)	0.4571 (4)	0.1256 (2)	0.022 (2)
C(3)	0.1319 (5)	0.3226 (4)	0.1201 (2)	0.026 (2)
C(4)	0	0.2762 (7)	0.0884 (4)	0.025 (3)
O(1)	0	0.6225 (4)	0.1596 (2)	0.031 (2)
O(3)	0.2555 (3)	0.2801 (3)	0.0886 (2)	0.033 (1)
N(2)	0.1570 (4)	0.5147 (3)	0.0669 (2)	0.021 (1)
N(4)	0	0.3025 (5)	0.0233 (3)	0.025 (2)
O(1W)	0	0.8885 (5)	0.1361 (3)	0.049 (2)
O(2W)	0.1836 (7)	0.6999 (6)	0.25	0.058 (2)
		Zn Complex		
Br(1)	0	0.0800 (2)	0.25	0.061 (1)
Br(2)	0	0	0	0.032 (1)
Zn	0	0.5	0	0.021 (1)
C(1)	0	0.5010 (9)	0.1576 (5)	0.025 (4)
C(2)	0.1352 (8)	0.4593 (6)	0.1281 (3)	0.022 (3)
C(3)	0.1312 (8)	0.3251 (6)	0.1202 (3)	0.025 (3)
C(4)	0	0.2808 (10)	0.0884 (5)	0.022 (4)
O(1)	0	0.6255 (6)	0.1610 (3)	0.034 (3)
O(3)	0.2555 (5)	0.2824 (5)	0.0892 (3)	0.033 (2)
N(2)	0.1616 (6)	0.5192 (5)	0.0694 (3)	0.020 (2)
N(4)	0	0.3111 (8)	0.0228 (4)	0.026 (3)
O(1W)	0	0.8909 (7)	0.1362 (4)	0.052 (3)
O(2W)	0.1843 (9)	0.7035 (9)	0.25	0.060 (4)

[a] $U_{eq} = {}^1/_3 \sum_i \sum_j U_{ij} a_i^* a_j^* \mathbf{a}_i \mathbf{a}_j$.

Table III. Bond Lengths (Å) of the $M(taci)_2^{2+}$ Complexes (M = Ni, Cu, Zn) with Estimated Standard Deviations in Parentheses

distance	Ni complex	Cu complex	Zn complex
M–N(2)	2.112 (3)	2.086 (4)	2.173 (6)
M–N(4)	2.136 (5)	2.322 (6)	2.217 (9)
C(1)–C(2)	1.524 (5)	1.522 (7)	1.510 (10)
C(1)–O(1)	1.417 (7)	1.432 (9)	1.425 (13)
C(2)–C(3)	1.523 (6)	1.548 (6)	1.544 (9)
C(2)–N(2)	1.478 (5)	1.459 (6)	1.487 (10)
C(3)–C(4)	1.514 (5)	1.517 (7)	1.511 (10)
C(3)–O(3)	1.430 (5)	1.436 (6)	1.443 (9)
C(4)–N(4)	1.495 (8)	1.460 (10)	1.491 (14)

and room temperature. Pulse ENDOR and ESEEM were performed at 10 K. The FAB$^+$–MS spectra were run on a VG ZAB VSEQ instrument. Test solutions were prepared by dissolving the samples in water and mixing the resulting solutions with a glycerol matrix prior to the introduction through the vacuum lock. C, H, and N analyses were performed by D. Manser, Laboratorium für Organische Chemie, ETH Zürich, Switzerland; thermogravimetric analyses were measured on a Perkin-Elmer TGA 7 thermobalance using a heating rate of 10 °C min^{-1}.

Materials. taci was prepared according to ref 4. $H_3taci(NO_3)_3$ was obtained by dissolving 1 equiv of taci in water followed by the addition of 3.1 equiv of aqueous HNO_3 and precipitating the product by the addition of CH_3OH. For the preparation of the metal complexes, $NiBr_2 \cdot 3H_2O$, $Ni(NO_3)_2 \cdot 6H_2O$, $CuBr_2$ (anhydrous), $Cu(NO_3)_2 \cdot 3H_2O$, $ZnBr_2$ (anhydrous), and $Zn(NO_3)_2 \cdot 6H_2O$ (from Fluka, Buchs, Switzerland) were used. The complexes were obtained by the addition of 5 mL of an aqueous 0.9 M metal bromide or metal nitrate solution to 10 mL of an aqueous 1 M taci solution. During the addition, the solid complexes precipitated. The yield was completed (≥80%) by cooling to 4 °C. The solids were then filtered off and recrystallized from hot water. Crystals with the composition $M(taci)_2Br_2 \cdot 4H_2O$ were suitable for X-ray analysis. Drying in vacuo yielded well-defined solids with a lower water content. Prolonged drying in vacuo over P_2O_5 finally resulted in the formation of the anhydrous $M(taci)_2Br_2$ and $M(taci)_2(NO_3)_2$. Satisfactory analytical data were obtained for $H_3taci(NO_3)_3$ and for the metal complexes (Table S1, supplementary material).

All other reagents were commercially available products of reagent grade quality.

X-ray Diffraction Studies. The data collection of $Ni(taci)_2Br_2 \cdot 4H_2O$, $Cu(taci)_2Br_2 \cdot 4H_2O$, and $Zn(taci)_2Br_2 \cdot 4H_2O$ was performed on a four-circle Picker-Stoe diffractometer with graphite-monochromatized Mo Kα radiation. Three standard reflections were checked at an interval of every 1 h; no significant decrease of intensities was noted. A face-indexed, numerical absorption correction was applied. The structure was solved by direct methods of Siemens SHELXTL PLUS (VMS)[7] and refined with anisotropic displacement parameters for all non-hydrogen atoms. A riding model with fixed isotropic displacement parameters of 0.05 Å^2 (Ni) or 0.08 Å (Cu, Zn) was used to calculate the positions of 24 hydrogen atoms. The full-matrix least-squares refinements were carried out by minimizing $\sum w(F_o - F_c)^2$. The crystallographic data are summarized in Table I, atom coordinates are listed in Table II, and selected bond lengths and a summary of bond angles are presented in Tables III and IV.

Potentiometric Measurements. Potentiometric titrations were carried out with a Metrohm 654 pH/mV meter, a Philips glass electrode, and an Ag/AgCl reference electrode, fitted with a salt bridge containing 0.1

---

(7) Sheldrick, G. M. *SHELXTL-PLUS 88. Structure Determination Software Programs*; Nicolet Instrument Corp.: Madison, WI, 1988.

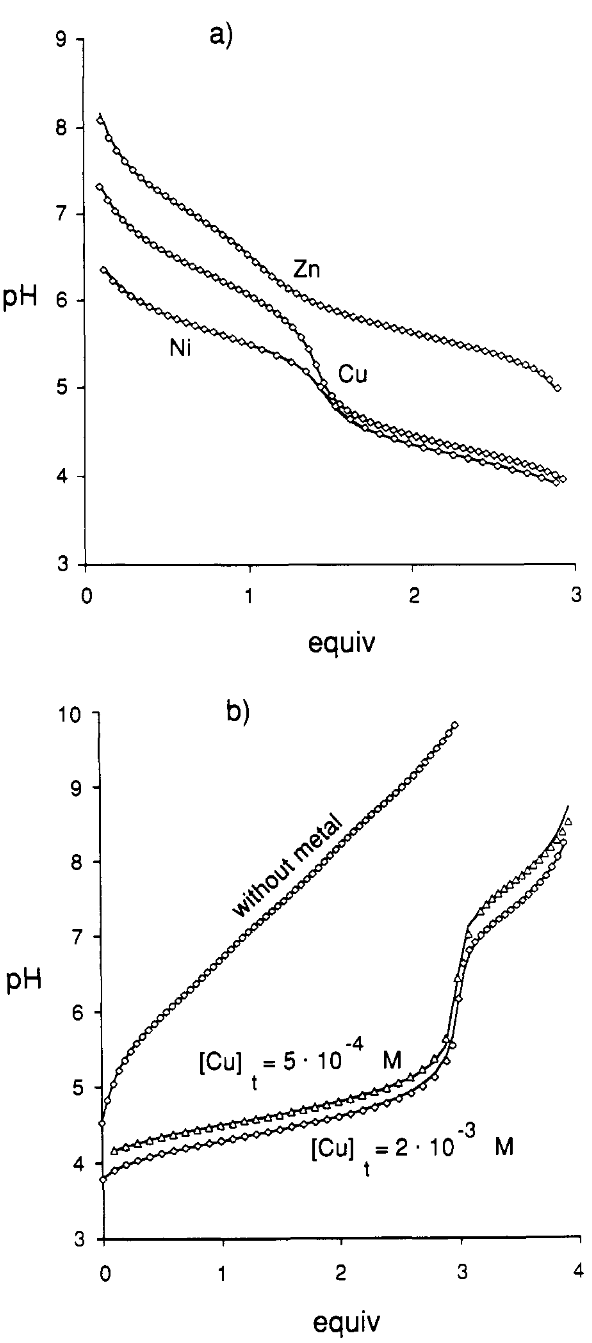

Figure 1. Titration (a) of $M(taci)_2Br_2$ (10^{-3} M) with 0.1 M HNO_3 and (b) of a 1:1 mixture of taci·3HNO_3 and $Cu(NO_3)_2$ with 0.1 M KOH (0.1 M KNO_3, 25 °C). The open squares represent experimental points; the solid lines were calculated from the equilibrium constants listed in Table V, equiv = moles of titrant per moles of taci.

M KNO_3. The sample solutions were titrated with 0.1 M KOH or 0.1 M HNO_3, dispensed from a Metrohm 665 piston buret. The ionic strength was adjusted to 0.1 M by adding appropriate amounts of KNO_3 to the test solutions. The potential measurements were performed in a water-jacketed beaker at 25 °C under an atmosphere of nitrogen (washed previously with an aqueous solution of 0.1 M KNO_3). The stability of the electrode system was checked by two calibration titrations prior and after each measurement. An evaluation of the obtained data was only performed if the difference in $E°$ was less than 0.5 mV. For calibration, 100 mL of 2 × 10^{-3} M HNO_3 was titrated with 0.1 M KOH and the potentials were corrected for phase-boundary effects caused by the high mobility of H^+ and OH^- according to the method given by Henderson.[8]

The pK determination of the ligand was performed by 12 alkalimetric titrations of analytically pure samples of $H_3taci(NO_3)_3$ (10^{-3} M or 2 × 10^{-3} M), which were free of stereoisomers according to its ^1H and ^{13}C NMR spectrum.

Table IV. Selected Bond Angles (deg) of the $M(taci)_2^{2+}$ Complexes (M = Ni, Cu, Zn) with Estimated Standard Deviations in Parentheses

angle	Ni complex	Cu complex	Zn complex
N(2)–M–N(4)	87.2 (1)	85.7 (2)	86.4 (2)
N(2)–M–N(2A)[a]	180.0 (1)	180.0 (1)	180.0 (1)
N(2)–M–N(2B)[a]	91.0 (2)	90.1 (2)	91.0 (3)
N(2)–M–N(2C)[a]	89.0 (2)	89.9 (2)	89.0 (3)
N(2)–M–N(4A)[a]	92.8 (1)	94.3 (2)	93.6 (2)
N(4)–M–N(4A)[a]	180.0 (1)	180.0 (1)	180.0 (1)
M–N(2)–C(2)	118.2 (2)	119.2 (3)	116.9 (4)
M–N(4)–C(4)	117.7 (3)	114.6 (4)	116.6 (7)

[a] Symmetry operations: (A) $-x$, $1 - y$, $-z$; (B) x, $1 - y$, $1 - z$; (C) $-x$, y, z.

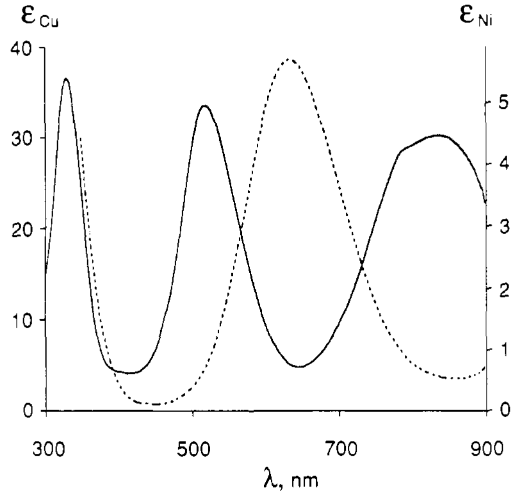

Figure 2. vis spectra of $Cu(taci)_2^{2+}$ (dotted line) and $Ni(taci)_2^{2+}$ (solid line) in H_2O.

Measurements with a metal to ligand ratio of 1:2 were performed by acidimetric titrations of solutions, containing 10^{-3} M of the complex, dissolved as crystalline, analytically pure $M(taci)_2Br_2$ or $M(taci)_2(NO_3)_2$ (M = Ni, Cu, Zn). Identical results were obtained for a given metal by using the complexes as nitrate or bromide. The reaction of $Ni(taci)_2^{2+}$ in the acidic range of the pH profile (pH ≤ 6) was too slow for a continuous titration. Therefore a batch method was applied, using 22 individually sealed and thermostated sample solutions. An appropriate amount of acid was added to each sample and was then allowed to equilibrate for 24 h.

Measurements with a ratio Cu to taci of 1:1 were performed by alkalimetric titrations of solutions containing analytically pure taci·3HNO_3 and $Cu(NO_3)_2$·3H_2O in a 1:1 ratio with $[Cu]_t$ of 2 × 10^{-3} and 5 × 10^{-4} M, respectively. The titration curves of the metal complexes are presented in Figure 1.

Calculations of Equilibrium Constants. All equilibrium constants were calculated as concentration constants.[9] The value for the ionic product of water (0.1 M KNO_3, 25 °C) was obtained from the calibration titration as pK_w = 13.79. The pK values of H_3taci were calculated from potentiometric data using the computer program PKAS.[9,10] The formation constants of the metal complexes were calculated by the computer program SUPERQUAD;[11] final refinements were performed, using the computer program BEST[9,12] for an optimal fit σ_{pH} (Table V). The calculations were carried out by varying all formation constants of the metal-containing species with fixed values for pK_w, the protonation constants of the ligand, and the concentrations of the reactants.

Results and Discussion

Preparation and Characterization of the Complexes. Crystalline samples of the solid complexes were easily obtained by the simple addition of aqueous solutions containing the metal as bromide or nitrate and the free ligand, respectively. Dehydration of crystalline

---

(8) Henderson, P. *Z. Phys. Chem.* **1907**, *59*, 118.

(9) Martell, A. E.; Motekaitis, R. J. *Determination and Use of Stability Constants*; VCH: New York, 1988.

(10) Motekaitis, R. J.; Martell, A. E. *Can. J. Chem.* **1982**, *60*, 168.

(11) Gans, P.; Sabatini, A.; Vacca, A. *J. Chem. Soc., Dalton Trans.* **1985**, 1195.

(12) Motekaitis, R. J.; Martell, A. E. *Can. J. Chem.* **1982**, *60*, 2403.

Table V. Potentiometric Data (25 °C, 0.1 M KNO_3) and Evaluated Equilibrium Constants for taci Complexes with Estimated Standard Deviations in Parentheses

	Ni^{2+}	Cu^{2+}			Zn^{2+}	H^+
		Experimental Data				
taci]$_t$:[M]$_t$:[H]$_t$	2:1:0	2:1:0	1:1:3	1:1:3	2:1:0	1:0:3
[taci]$_t$, moles dm^{-3}	2×10^{-3}	2×10^{-3}	2×10^{-3}	5×10^{-4}	2×10^{-3}	2×10^{-3}
titrant; [titrant], moles dm^{-3}	HNO_3; 0.1	HNO_3; 0.1	KOH; 0.1	KOH; 0.1	HNO_3; 0.1	KOH; 0.1
evaluated range[a]	0.1–2.90	0.1–2.90	0.05–3.95	0.1–3.90	0.1–2.90	0.1–2.90
no. of points	38	61	49	45	57	57
		Equilibrium Constants				
log β_1[b]	12.37 (1)	12.09 (1)	12.10 (2)	12.05 (2)	8.40 (1)	pK_1 = 5.95[c]
log β_2[b]	20.94 (1)	18.79 (1)			13.56 (1)	pK_2 = 7.40[c]
log β_{HML_2}[d]		24.60 (2)				pK_3 = 8.90[c]
log β_D[e]			12.0 (1)	11.8 (1)		
σ_{pH}[f]	0.0056	0.0017	0.0046	0.0077	0.0043	0.0021

[a] Moles of titrant per moles of taci. [b] $\beta_i = [M(taci)_i]/([M][taci]^i)$. [c] $K_i = [H_{3-i}taci][H]/[H_{4-i}taci]$, estimated standard deviations <0.01. [d] $\beta_{HML_2} = [M(taci)(Htaci)]/([M][taci]^2[H])$. [e] $\beta_D = [M_2(taci)_2(OH)_2][H]^2/([M]^2[taci]^2)$. [f] $\sigma_{pH} = (\sum w(pH_{obs} - pH_{calcd})^2/\sum w)^{1/2}$, $w = (pH_{i+1} - pH_{i-1})^{-2}$.

$M(taci)Br_2 \cdot 4H_2O$ was investigated by thermogravimetry. A decrease of 10–11% of the sample weight in the range 60–130 °C indicated a complete dehydration of all three compounds. Thermogravimetric curves and their first derivatives are available as supplementary material. The structure of the three complexes was elucidated by spectroscopic methods. The vis spectrum of the pink $Ni(taci)_2^{2+}$ complex indicated unambiguously the presence of an octahedral NiN_6 chromophore (Figure 2).[13] Solutions, containing Ni and taci in a 1:1 ratio showed a deep blue color, indicating the formation of $Ni(taci)(H_2O)_3^{2+}$. However, solid compounds of this composition have not been isolated yet. A tetragonal distorted CuN_6 coordination sphere was elucidated for $Cu(taci)_2^{2+}$ by EPR spectroscopy. At room temperature, a resonance with $g_\parallel = 2.246$, $g_\perp = 2.078$, and $A_\parallel^{Cu} = 145 \times 10^{-4}$ cm^{-1} was observed. These values shifted to $g_\parallel = 2.262$, $g_\perp = 2.055$, and $A_\parallel^{Cu} = 172 \times 10^{-4}$ cm^{-1} at 4 K. This result corresponds well with the structurally related $Cu(tach)_2(ClO_4)_2$ (tach = *all-cis*-1,3,5-triaminocyclohexane): $g_\parallel = 2.25$, $g_\perp = 2.05$, and $A_\parallel^{Cu} = 176 \times 10^{-4}$ cm^{-1} (80 K).[14] The coupling to the four equatorial nitrogen atoms was observed in the pulse ENDOR spectrum, $A_\perp^N = 32$ MHz, $A_\parallel^N = 27$ MHz, and the electron-spin-echo envelope modulation (ESEEM) showed the coupling to the axial nitrogen atoms with NMR frequencies in the range 0.5–8 MHz. Peisach and Blumberg discussed the dependence of $A_\parallel^{Cu}$ on $g_\parallel$ as a function of the coordination sphere of Cu.[15] Such relations are useful to identify the binding of Cu in proteins. The parameters, observed at 4 K do fall in the range postulated for a complex with four equatorial nitrogen atoms. However, no accordance with the Peisach–Blumberg relation was observed at room temperature. This is particularly a consequence of the significant temperature dependence of $A_\parallel^{Cu}$. On the other hand, the ^{14}N hyperfine coupling (ENDOR) of $Cu(taci)_2^{2+}$ was in excellent agreement with the range expected for Cu, ligated by four sp^3 nitrogen atoms.[16] For $Zn(taci)_2^{2+}$, ^1H NMR and ^{13}C NMR spectroscopy was most effective for structural characterization. The presence of two signals in the ^1H NMR (2 × 3 H) as well as in the ^{13}C NMR spectrum demonstrated D_{3d} symmetry for the complex. Moreover, in the course of coordination, a significant shift for the signals was observed in the ^1H NMR spectrum (free ligand 3.83 and 2.80 ppm; Zn complex 3.87 and 3.60 ppm). The signal at 2.8 ppm in the spectrum of the free ligand corresponds to the proton on C(–N). An assignment of the signals in the complex is not quite clear. However, the large shift of H–C(–N) clearly indicated the binding of Zn to the three nitrogen atoms of taci.

Crystal Structure of $M(taci)_2Br_2 \cdot 4H_2O$ (M = Ni, Cu, Zn). The three compounds are isomorphous and crystallize in the centrosymmetric space group *Cmcm*. The two Br^- ions have different environments. Br(1) is coordinated to four water molecules by hydrogen bonding, whereas Br(2) is located in a cavity, formed by six NH_2 groups of two ligand molecules and two water molecules (Figure 3). The coordination sphere of the metal is roughly octahedral, subjected to a tetragonal and a trigonal distortion. The combination of the two distortions resulted in the crystallographic symmetry C_{2h}. The trigonal distortion can be seen by the angles N–M–N < 90° and N–M–N′ > 90° (N and N are two atoms of the same ligand, N and N′ are atoms of two different ligands) and must be regarded as a stretching along the pseudo-3-fold axis. It is obviously a consequence of the ligand geometry. The tetragonal distortion is expressed by a longer distance M–N(4) compared to M–N(2) and can be regarded as a stretching along the pseudo-4-fold axis. As expected, the tetragonal distortion *T* of the Ni and Zn complex is marginal ($T_{Ni} = 0.989$, $T_{Zn} = 0.980$) compared to Cu ($T_{Cu} = 0.898$); *T* is defined as the ratio

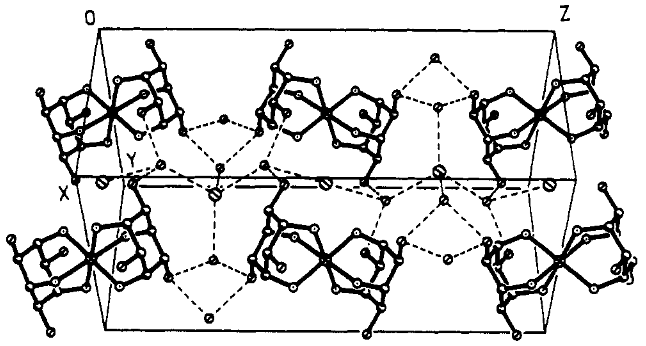

Figure 3. Unit cell of $M(taci)_2Br_2 \cdot 4H_2O$ (M = Ni, Cu, Zn). The parameters drawn refer to the Cu complex.

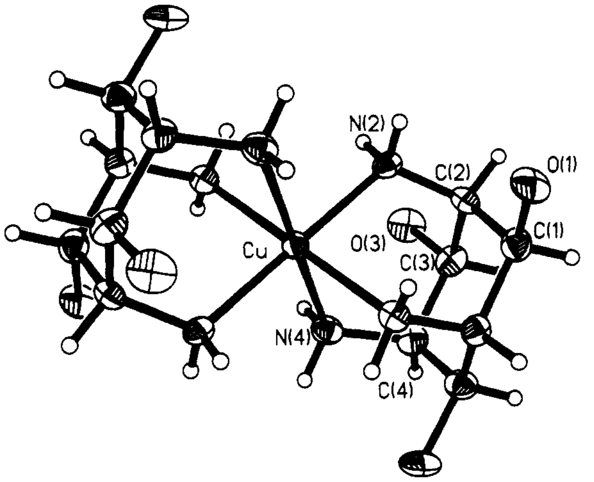

Figure 4. Drawing of $[M(taci)_2]^{2+}$ (M = Ni, Cu, Zn) with numbering scheme and vibrational ellipsoids at the 50% probability level. The parameters drawn refer to the Cu complex.

---

(13) Urbach, F. L.; Sarneski, J. E.; Turner, L. J.; Busch, D. H. *Inorg. Chem.* **1968**, *7*, 2169.

(14) Childers, R. F.; Wentworth, R. A. D.; Zompa, L. J. *Inorg. Chem.* **1971**, *10*, 302.

(15) Peisach, J.; Blumberg, W. E. *Arch. Biochem. Biophys.* **1974**, *165*, 691.

(16) Iwaizumi, M.; Kudo, T.; Kita, S. *Inorg. Chem.* **1986**, *25*, 1546.

Table VI. FAB$^+$ Mass Sepctrometry Data for $M(taci)_2Br_2$ (Glycerol Matrix), Relative Intensities of Major Metal-Containing Ions

	% Ni	% Cu	% Zn
$H_{-1}M(taci)^+$	22	<5	38
$M(taci)^+$	59	100	28
$M(taci)Br^+$	40	12	100
$H_{-1}M(taci)_2^+$	100	21	80
$M(taci)_2^+$	15	6	7
$M(taci)_2Br^+$	29	10	17

of the mean in-plane M–N bond length to the mean out-of-plane M–N bond length.[17] A view of the $Cu(taci)_2^{2+}$ complex is given in Figure 4. As shown by NMR data, the symmetry of the Zn complex in solution is fully D_{3d}. There is good reason to expect the same behavior for the Ni complex. Thus, the tetragonal distortion of the Ni and the Zn complexes must be interpreted as a consequence of the crystal packing. However, the large tetragonal distortion of the Cu complex is in agreement with the usual Jahn-Teller distortion, observed for many Cu(II) compounds.

Even though the X-ray scattering abilities of nitrogen and oxygen do not differ widely, an unambiguous determination of the structure ensued from the differences in the C–O and C–N bond lengths[4] and from the higher electron density values at the oxygen positions compared with the nitrogen positions. In addition, a comparison with M–N and M–O bond distances of structurally related complexes provided strong evidence for an MN_6 geometry (Table III).[18] Typical mean bond lengths for complexes with a related coordination sphere are Ni–O 2.05–2.08 Å, Ni–N 2.11–2.13 Å, Cu–O 1.94–1.98 Å, Cu–N 2.01–2.08 Å, Zn–O 2.07–2.10 Å, and Zn–N 2.17–2.22 Å.[19]

Mass Spectrometry. Owing to the multiisotopic nature of Ni, Cu, and Zn, the signals of metal-containing species could be easily recognized in each spectrum. A set of monopositive ions was observed by using the fast atom bombardment (FAB$^+$) method; assignments of the major peaks are summarized in Table VI. Monopositive ions were generated from $M(taci)^{2+}$ and $M(taci)_2^{2+}$ by three distinct processes: (i) aggregation or coordination of Br^-, (ii) dissociation of H^+, and (iii) electron uptake. All three processes may be interpreted as chemical reactions in the glycerol matrix. It is reasonable to regard $M(taci)Br^+$ as a 4-fold coordinated complex whereas $M(taci)_2Br^+$ should rather be considered as an outer-sphere ion aggregate. The observed loss of H^+ indicates obviously a deprotonation of one of the equatorial OH groups in taci. We recently discussed the enhanced acidity for alcoholic groups in this molecule.[4] The electron uptake corresponds to the reduction of M(II) to M(I). It is well-known that the glycerol matrix acts readily as a reducing agent under FAB conditions.[20] Although the spectra of the three compounds are essentially the same, the individual properties of Ni(II), Cu(II), and Zn(II) are clearly expressed by a different intensity distribution of the observed peaks. $Zn(taci)Br^+$ is the most intense peak in the spectrum of the Zn complex and shows the high tendency of Zn(II) to form tetrahedral species. On the other hand, $Cu(taci)^+$ dominates the spectrum of the Cu complex, demonstrating the easy reducibility of Cu(II). The high tendency of Ni(II) for octahedral complexes is indicated by the favored formation of $H_{-1}Ni(taci)_2^+$.

Equilibria in Aqueous Media. The stability constants for ligand protonation and complex formation are summarized in Table V.

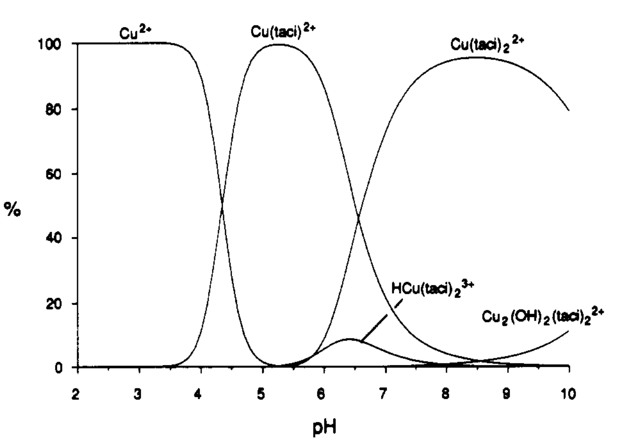

Figure 5. Species distribution of equilibrated aqueous solutions with Cu:taci = 1:2, $[Cu]_t = 10^{-3}$ M. The species concentrations were calculated with the equilibrium constants listed in Table V.

The titration curves of the 1:2 complexes (Figure 1a) were used to calculate the formation constants of $M(taci)^{2+}$ and $M(taci)_2^{2+}$. For the Ni and Zn complex, this model was in good agreement with the experimental data. However, small but systematic deviations $pH_{calc} - pH_{obs} \leq 0.05$ were observed in the pH profile of the Cu complex, particularly in the range where $Cu(taci)^{2+} + taci \rightleftharpoons Cu(taci)_2^{2+}$ is the predominant reaction. These deviations obviously indicated the presence of additional species in the equilibrium system. The formation of either hydroxo complexes $Cu_n(taci)_n(OH)_n^{n+}$ or a protonated species $H_nCu(taci)_2^{(n+2)+}$ was therefore taken into consideration. The first hypothesis was checked by evaluating the data from the alkalimetric titration of $Cu(taci)^{2+}$ (Figure 1b). The observation of a second buffer region 3 < equiv < 4 clearly confirmed the formation of a hydroxo complex with Cu:taci:OH = 1:1:1. A significant dependence of the midpoint potential at equiv = 3.5 on $[Cu]_t$ and a rather slow equilibrium (up 10 min for constant pH) indicated a consecutive reaction following the deprotonation of one coordinated water molecule. Therefore, two additional species were postulated:

$$Cu(taci)^{2+} \rightleftharpoons Cu(taci)(OH)^+ + H^+ \qquad \text{(i)}$$

$$K_{OH} = [Cu(taci)(OH)^+][H^+]/[Cu(taci)^{2+}]$$

$$nCu(taci)(OH)^+ \rightleftharpoons Cu_n(taci)_n(OH)_n^{n+} \qquad \text{(ii)}$$

$$K_{poly} = [Cu_n(taci)_n(OH)_n^{n+}]/[Cu(taci)(OH)^+]^n$$

Our data did not allow the unambiguous determination of the nuclearity n. However, the most consistent evaluation for the two titration curves with $[Cu]_t = 2 \times 10^{-3}$ M and $[Cu]_t = 5 \times 10^{-4}$ M revealed a dinuclear complex with the overall formation constant $\beta_{poly} = [Cu_2(taci)_2(OH)_2^{2+}][H^+]^2/([Cu^{2+}]^2[taci]^2) = 8 \times 10^{11}$. SUPERQUAD[11] rejected the consideration of the corresponding mononuclear expressed by $\beta_{OH} = [Cu(taci)(OH)^+][H^+]/([Cu^{2+}][taci])$. Only a rough estimation $3.6 \leq \log \beta_{OH} \leq 4.0$ can be given. Therefore, $8.0 \leq -\log K_{OH} \leq 8.4$ and $4.0 \leq K_{poly} \leq 4.8$, $n = 2$, are appropriate values for the two equilibria (i) and (ii).

By use of the evaluated formation constant β_{poly}, the dinuclear hydroxo complex did not sufficiently appear in the titration of the 1:2 complex to explain the above mentioned deviation (Figure 5). However, the deviation disappeared by admitting the protonated complex $HCu(taci)_2^{3+}$. It should be noted that $HCu(taci)_2^{3+}$ is only a minor species. Its concentration never exceeds 10% of the equilibrium composition (Figure 5). Thus the value of the formation constant of $HCu(taci)_2^{3+}$ as presented in Table V is rather poorly defined.

Conclusions

A summary of the formation constants of taci and some other saturated polyamines is given in Table VII. This comparison

---

(17) Hathaway, B. J.; Hodgson, P. G. *J. Inorg. Nucl. Chem.* **1973**, *35*, 4071.

(18) Ammeter, J. H.; Bürgi, H. B.; Gamp, E.; Meyer-Sandrin, V.; Jensen, W. P. *Inorg. Chem.* **1979**, *18*, 733.

(19) Minima and maxima of the averaged values $^1/_6\sum d(M-X)$ for a total of 39 octahedral NiO_6, NiN_6, ZnO_6, and ZnN_6 complexes were obtained from the Cambridge Structural Database. For Cu, a total of 17 tetragonal distorted CuO_6 and CuN_6 complexes was used and only the short bonds to the equatorial ligands were considered according to $^1/_4\sum d(M-X_{eq})$.

(20) (a) Kyranos, J. N.; Vouros, P. *Biomed. Environ. Mass Spectrom.* **1990**, *19*, 628. (b) Věkey, K. *Int. J. Mass Spectrom. Ion Processes* **1990**, *97*, 265. (c) Kazakoff, C. W.; Rye, R. T. B. *Org. Mass Spectrom.* **1991**, *26*, 154. (d) Agnello, A.; De Pauw, E. *Org. Mass Spectrom.* **1991**, *26*, 175.

(21) Prue, J. E.; Schwarzenbach, G. *Helv. Chim. Acta* **1950**, *33*, 985.

Table VII. Comparison of Protonation, log K_i^H, and Complex Formation, log K_i^M, of Selected Aliphatic or Alicyclic Triamines[a]

	H^+			Ni^{2+}		Cu^{2+}		Zn^{2+}	
	K_1	K_2	K_3	K_1	K_2	K_1	K_2	K_1	K_2
den[b]	9.9	9.1	4.3	10.7	8.2	16.0	5.3	8.9	5.5
dpt[c]	10.7	9.6	7.7	9.2	3.6	14.2		7.9	
ptn[d]	9.6	8.0	3.7	9.3		11.1		6.7	
tame[e]	10.2	8.3	5.9	10.1	7.2	11.0	7.7	6.6	4.3
tach[f]	10.2	8.7	7.2	9.9		10.6		6.9	
[9]aneN_3[g]	12.6	7.2		16.2		17.5	14.0	11.6	
[12]aneN_3[g]	13.2	8.0		10.9		13.2	7.7	8.8	
taci[h]	8.9	7.4	6.0	12.3	8.6	12.1	6.7	8.4	5.2

[a] Protonation constants are listed as log ($[H_iL][H_{i-1}L]^{-1}[H]^{-1}$), $1 \leq i \leq 3$; complex formation constants are listed as log ($[ML_i][ML_{i-1}]^{-1}[L]^{-1}$), $1 \leq i \leq 2$. [b] 1,5-Diamino-3-aza-pentane (0.1 M KCl, 20 °C, ref 21). [c] 1,7-Diamino-5-aza-heptane (0.1 M KCl, 25 °C, ref 22). [d] 1,2,3-Triaminopropane (0.1 M KCl, 20 °C, ref 23). [e] Tris(aminomethyl)ethane (0.5 M KNO_3, 25 °C, ref 24). [f] *All-cis*-1,3,5-triaminocyclohexane (0.1 M KCl 25 °C, ref 14). [g] 1,4,7-Triazacyclononane and 1,5,9-triazacyclododecane (Ni, Zn: 0.1 M KNO_3, 25 °C, ref 25; all other 0.5 M KNO_3, 25 °C, ref 26). [h] 1,3,5-Triamino-1,3,5-trideoxy-*cis*-inositol (0.1 M KNO_3, 25 °C, this work).

Scheme I

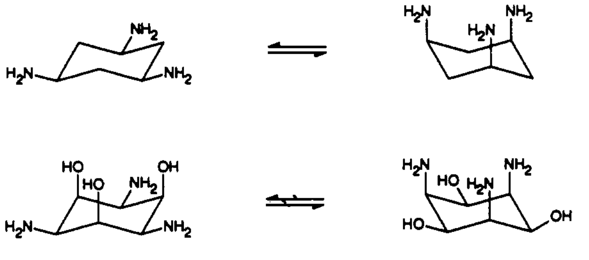

demonstrates that taci is an effective chelator for Ni(II). Actually only 1,4,7-triazacyclononane forms more stable Ni(II) complexes than taci. Particular attention deserves the structurally related *all-cis*-triaminocyclohexane (tach). Both ligands provide a rigid arrangement of three amino groups which are sterically constrained to a facial coordination. The significantly higher stability constants of taci–metal complexes are in contrast with the somewhat lower affinity of taci for H^+. As long as the two ligands do not interact with a metal, an equatorial arrangement of the three amino groups is the predominant conformation (Scheme I)

In the case of tach, the required chair conversion provokes additional 1,3-diaxial repulsion. Since both conformations of taci are destabilized by such interactions, the difference of energy between the two conformations is much smaller. As a consequence the metal complexes of taci are more stable and the kinetic of formation is much faster. For example, it has been reported that the combination of solutions containing tach and Ni^{2+} in a 2:1 ratio resulted in the formation of solid $Ni(OH)_2$ and that the final equilibrium, involving essentially $Ni(tach)_2^{2+}$, was only reached after several days.[14,27] In contrast, the Ni(II) complex of taci is formed instantly by the mixing of the two solutions. The lower affinity of taci for H^+ may be considered to reflect the electron-withdrawing properties of the three additional hydroxyl groups.

Chart III

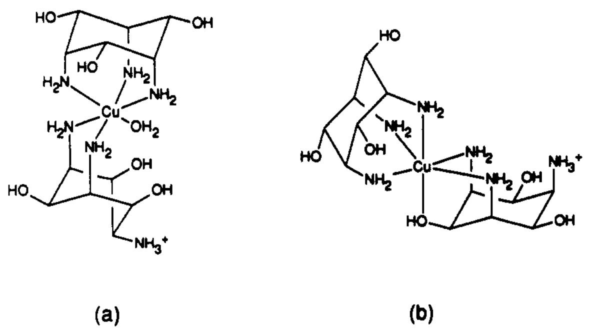

(a) (b)

It is obvious that taci is not as powerful in chelating Cu(II) and Zn(II). Both metals have a smaller tendency to form octahedral complexes, and the steric flexible den forms a more stable Zn(II) and Cu(II) complex than taci. The observed permutation of the usual Irving Williams order for Ni(II) and Cu(II) is obviously a consequence of the rigid ligand geometry which resists the tetragonal Jahn-Teller distortion. With respect to the favored 4 + 2 coordination of Cu(II), we actually expected the coordination of Cu(II) to site ii (Chart I), forming two short Cu–N and one long Cu–O bond. However, the results presented in this paper clearly refute this assumption for $Cu(taci)^{2+}$ and $Cu(taci)_2^{2+}$ in the solid state and in solution. No structural data are available for the postulated $HCu(taci)_2^{3+}$. It seems quite clear that one of the amino groups is protonated and therefore not coordinated to Cu(II). From the two suggestions, given in Chart III, structure b providing an CuN_5O coordination sphere with an elongated Cu–O bond seems more reasonable.

Acknowledgment. We thank Arthur Schweiger and Walter Lämmler for the measurements of the EPR spectra, Martin Colussi for the performance of the thermogravimetric analyses, Ruth Blumer for NMR measurements, Rolf Häfliger for the recording of the FAB-MS spectra, and Lorenza Primo and Tiziana Mordasini for practical assistance in the X-ray measurements. Financial support by the ETHZ, Kredite für Unterricht and Forschung, Project No. 08099/41-0410.5, for M.G. and by the Laboratorien Hausmann AG, St. Gallen, Switzerland, for H.S. is gratefully acknowledged.

Supplementary Material Available: Table S1, listing analytical data, Tables SII–SV, listing crystallographic data, anisotropic displacement parameters, positional parameters of hydrogen atoms, and bond angles, and Figures S1–S7, showing the FAB^+-MS and thermogravimetric analyses of $M(taci)_2Br_2$ (M = Ni, Cu, Zn) and the EPR spectrum of $Cu(taci)_2Br_2$ (19 pages); tables of calculated and observed structure factors (9 pages). Ordering information is given on any current masthead page.

---

(22) Vacca, A.; Arenare, D.; Paoletti, P. *Inorg. Chem.* **1966**, *5*, 1384.
(23) Prue, J. E.; Schwarzenbach, G. *Helv. Chim. Acta* **1950**, *33*, 995.
(24) (a) Sabatini, A.; Vacca, A. *J. Chem. Soc., Dalton Trans.* **1980**, 519. (b) Sabatini, A.; Vacca, A. *Coord. Chem. Rev.* **1975**, *16*, 161.
(25) (a) Yang, R.; Zompa, L. J. *Inorg. Chem.* **1976**, *15*, 1499. (b) Zompa, L. J. *Inorg. Chem.* **1978**, *17*, 2531.
(26) Riedo, T. J.; Kaden, T. A. *Helv. Chim. Acta* **1979**, *62*, 1089.
(27) Brauner, P. A.; Schwarzenbach, G. N. *Helv. Chim. Acta* **1962**, *45*, 2030.